Stoichiometry dependence and thermal stability of conducting NdGaO3/SrTiO3 heterointerfaces

F. Gunkel, K. Skaja, A. Shkabko, R. Dittmann, S. Hoffmann-Eifert et al.

Citation: Appl. Phys. Lett. **102**, 071601 (2013); doi: 10.1063/1.4792509
View online: http://dx.doi.org/10.1063/1.4792509
View Table of Contents: http://apl.aip.org/resource/1/APPLAB/v102/i7
Published by the American Institute of Physics.

Stoichiometry dependence and thermal stability of conducting $NdGaO_3/SrTiO_3$ heterointerfaces

F. Gunkel,[a] K. Skaja, A. Shkabko, R. Dittmann, S. Hoffmann-Eifert, and R. Waser
Peter Gruenberg Institute, Forschungszentrum Juelich GmbH and Juelich Aachen Research Alliance for Fundamentals on Future Information Technology (JARA-FIT), 52425 Juelich, Germany

(Received 10 October 2012; accepted 4 February 2013; published online 19 February 2013)

The structural and electrical properties of conducting $NdGaO_3/SrTiO_3$ (NGO/STO) heterostructures grown at various deposition temperatures were investigated. X-ray diffraction and X-ray photoelectron spectroscopy reveal a strong impact of the growth temperature on both crystallinity and cation stoichiometry of the NGO thin films. This stoichiometry variation significantly affects the electrical properties of the NGO/STO interface. High temperature conductance measurements under oxygen equilibrium conditions show a distinct conductance contribution of the NGO/STO interface up to 1000 K and exclude a conduction effect caused by a mere reduction of the STO substrate. Above 1000 K, the interface conduction is degrading due to a thermal instability. Both stoichiometry variation in as-grown films and thermal instability are attributed to the preferential evaporation of gallium from the NGO thin films at elevated temperatures. © *2013 American Institute of Physics*. [http://dx.doi.org/10.1063/1.4792509]

Conducting interfaces between insulating perovskite oxides have been subject of many recent studies. In particular, the interface between $LaAlO_3$ (LAO) and $SrTiO_3$ (STO)[1] has been investigated intensively. The most popular model to explain the electronic charge carriers at the interface is an electronic reconstruction resulting from the polar nature of LAO.[2] However, crystal imperfections and defects at the interface such as oxygen vacancies[3,4] and cation intermixing[2,5] have been identified to significantly influence the interface conductivity as well. In addition, an effect of acceptor-type Sr vacancies reducing the interfacial carrier density has been proposed.[6] For a better understanding of these interface effects, it is important to find alternative perovskite systems with similar properties next to LAO/STO. To date, most compounds which have been successfully tested to form a conducting interface with STO, i.e., $LaAlO_3$,[1] $LaGaO_3$,[7] and $LaVaO_3$,[8] contain La^{3+} as A-site cation of the polar perovskite material. Just recently, interfacial conductivity has been reported for $NdGaO_3$(NGO)/STO heterostructures.[9] NGO crystallizes in the orthorhombic space group Pbnm. The distorted perovskite structure of NGO can be described as a pseudo-cubic system with a lattice spacing of $d_{110} = 3.86$ Å. The pseudo-cubic lattice consists of an alternating stack of charged $(NdO)^+$ and $(GaO_2)^-$ planes. Therefore, it can be regarded as a polar perovskite material with Nd^{3+} as A-site cation.

In this study, the influence of the NGO cation stoichiometry on the interfacial conductivity of NGO/STO heterostructures is addressed. In particular, the role of the B-site cation, Ga^{3+}, will be discussed. One focus is the effect of the growth temperature on both the crystallinity and the stoichiometry of the deposited NGO layers. As will be shown, the Ga content in the NGO films can be controlled by the choice of a suitable growth temperature with significant effect on the conductance of the NGO/STO interface. Moreover, *in situ* measurements of the high temperature equilibrium conductance (HTEC) under various oxygen partial pressures (pO_2) provide information on the conduction mechanism at the NGO/STO interface. At the same time, the high temperature experiments are exploited to probe the thermal stability of the NGO/STO heterostructures.

NGO/STO heterostructures were obtained by pulsed laser deposition (PLD) of NGO on TiO_2-terminated (001) STO substrates. The NGO thin films were grown at temperatures between 920 K and 1070 K and at an oxygen partial pressure of 4×10^{-5} mbar. Laser fluence and ablation frequency were set to $1.4\,J/cm^2$ and 1 Hz, respectively. After the growth, the heterostructures were cooled down to room temperature at a constant rate of 10 K/min in deposition atmosphere. The growth procedure was monitored by reflection high energy electron diffraction (RHEED). The electrical properties of the NGO/STO heterostructures were investigated in a van der Pauw configuration, while the NGO/STO interface was contacted by ultrasonic Al wire bonding. X-ray photoelectron spectroscopy (XPS) analyses were performed with a PHI 5000 Versa Probe. For a stoichiometry determination of the NGO thin films, the Nd 4d and Ga 2p spectral lines were recorded. The data were quantified using PHI MultiPak 9.3

Fig. 1 summarizes RHEED data and X-ray diffraction (XRD) data for 20 unit cells (uc) thick NGO films grown at deposition temperatures (T_{dep}) of 920 K, 970 K, 1020 K, and 1070 K. The RHEED intensity signal recorded during the growth (Fig. 1(a)) evidences a clear impact of T_{dep} on the growth process. For all temperatures, intensity oscillations are observed indicating a layer-by-layer growth mode. However, amplitude and damping of the oscillations strongly depend on the growth temperature. Starting at $T_{dep} = 920$ K, clear oscillations with almost constant amplitude were observed after an initial intensity decay. Increasing T_{dep} to 970K improves both the amplitude and the stability of the RHEED oscillations. However, at even higher deposition temperatures, the RHEED oscillations show a strong damping leading to a constant intensity signal after the growth of approximately 15 uc. Moreover, the diffraction patterns received after the growth change with T_{dep} (Fig. 1(b)). The distinct reflection and diffraction spots observed

[a]f.gunkel@fz-juelich.de.

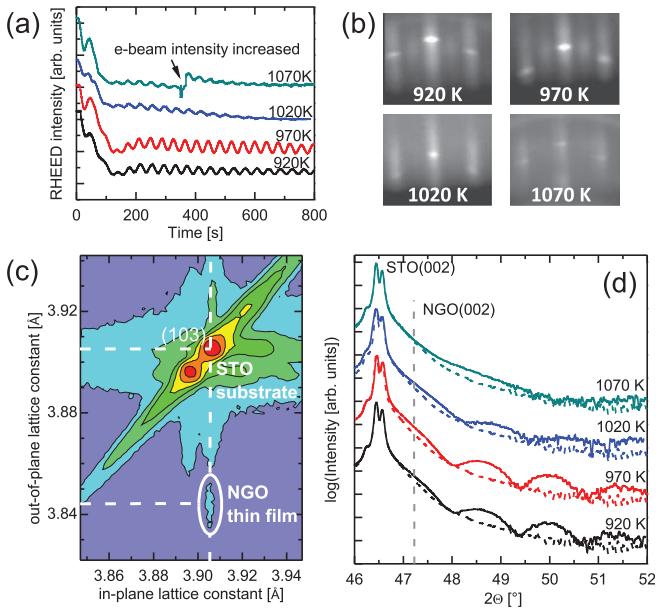

FIG. 1. Structural analyses of 20 uc thick NGO films grown at various deposition temperatures; (a) RHEED intensity recorded during the growth and (b) corresponding final diffraction patterns; (c) (103)-reciprocal space map for the sample grown at 970 K; (d) $(\Theta - 2\Theta)$ scans around the (002) STO substrate peak. (The dashed lines denote the STO substrate only.)

for $T_{dep} = 920$ K and 970 K become weaker for 1020 K and almost disappear for 1070 K, indicating an increasing surface roughness of the NGO thin films with increasing T_{dep}. In the diffraction patterns of the samples grown at 920 K and 970 K, additional streaks are observed between the ± 01 reflections and the specular spot. According to Ref. 9, this can be attributed to a c(2×2) reconstruction associated with the orthorhombic distortion of the NGO unit cell. The thicknesses of the NGO layers were estimated by X-ray reflectivity (XRR) measurements yielding values between 7.2 nm and 7.8 nm for the four nominally 20 uc samples. Moreover, the lattice parameters of the NGO layers were determined using reciprocal space mapping. As demonstrated for $T_{dep} =$ 970 K (Fig. 1(c)), the heteroepitaxial NGO film grows fully strained in-plane. As a consequence, the out-of-plane lattice constant is shortened to $c_{film} \simeq 3.845$ Å due to the tensile in-plane strain. The corresponding position of the pseudo-cubic (002) NGO peak is marked in the $(\Theta - 2\Theta)$ scans around the (002) STO substrate peak shown in Fig. 1(d). The main film peaks are hardly resolved in the $(\Theta - 2\Theta)$ scans due to the small thickness of the NGO layers. The samples grown at 920 K and 970 K show the most pronounced thickness fringes. However, for the samples grown at higher T_{dep}, much weaker and broadened thickness oscillations are observed. For the sample grown at 1070 K, thickness fringes are almost absent. However, a weak trace of a residual crystalline NGO layer is still evident. Thus, the crystal quality is significantly decreased at higher deposition temperatures. Moreover, the thickness of the crystalline portion of the deposited films seems to decrease with increasing growth temperatures >970 K as indicated by the broadening of the thickness oscillations, while the total thickness of the deposited layers is comparable for all samples according to XRR.

Fig. 2(a) shows the Ga/Nd ratio of the NGO films obtained from XPS probing the topmost nanometers of the NGO layer. As a reference for a stoichiometric composition (Ga/Nd = 1), a NGO single crystal was used. The Ga content in the NGO thin films decreases constantly with increasing T_{dep}, whereas the Nd content remains unaffected. As a result, the Ga/Nd ratio decreases constantly with increasing deposition temperature (from Ga/Nd = 0.93 for $T_{dep} = 920$ K to Ga/Nd = 0.10 for $T_{dep} = 1070$ K). Hence, the variation of the growth temperature results in a strong variation of the cation stoichiometry of the NGO films. As a consequence, the observed variation of the film crystallinity mainly can be attributed to a stoichiometry effect. For NGO single crystals, Ga tends to evaporate at sufficiently high temperatures (above 1100 K).[10,11] Therefore, we suppose that also the NGO thin films suffer from a loss of Ga due to thermal evaporation during film growth and subsequent cooling. Since the Ga vapor pressure increases with increasing temperature, this effect is expected to be more pronounced for increased deposition temperatures in accordance with the observed decrease of the Ga/Nd ratio.

As tested for the growth temperature of 970 K, the NGO/STO heterostructures show a metallic conductivity above a critical layer thickness of 4 uc similar to LAO/STO (Ref. 12) and $LaGaO_3$/STO.[7] At 5 K, the mobility reaches values of about 1000 cm^2/Vs, which is one order of magnitude higher than the first reported value for NGO/STO heterostructures.[9] In agreement with Ref. 9, the electron mobility is proportional to T^{-2} above 50 K, which indicates a strong electron-electron interaction. At 300 K, the sheet carrier density n_S is about 1×10^{14} cm^{-2}, which is well below the critical carrier densities observed for a bare reduction of the STO substrate.[3,13]

Figs. 2(b)–2(d) present room temperature Hall data for 8 uc and 20 uc thick NGO films grown at various deposition temperatures. The room temperature sheet resistance of the

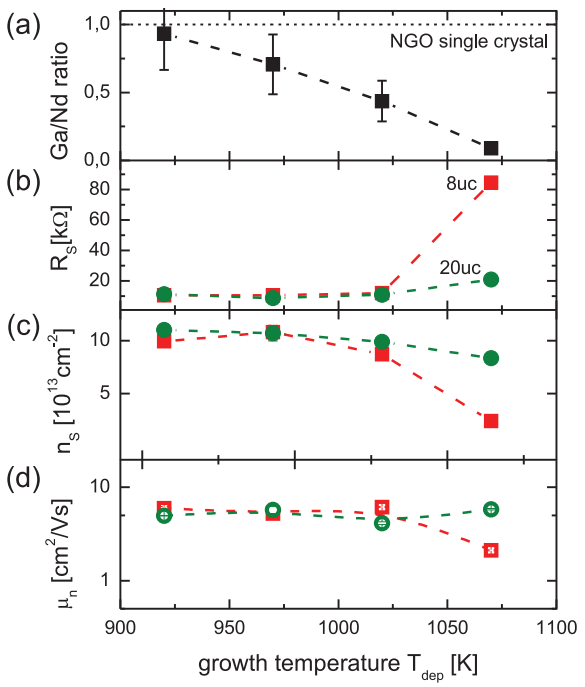

FIG. 2. Stoichiometry of NGO thin films grown at various deposition temperatures in comparison to their electrical properties; (a) Ga/Nd ratio; (b) sheet resistance of 8 uc (squares) and 20 uc (circles) thick NGO layers on STO; (c) corresponding carrier density and (d) mobility at 300 K.

NGO/STO heterostructures, R_S (Fig. 2(b)), shows a dependence on T_{dep} indicating a correlation between the NGO cation stoichiometry and the NGO/STO interface conductivity. For growth temperatures between 920 K and 1020 K, R_S varies slightly with a minimum for $T_{dep} = 970$ K. Moreover, no significant thickness dependence is observed for these growth temperatures and the related stoichiometry range. However, towards higher growth temperatures, the sheet resistance of the NGO/STO heterostructures increases and shows a dependence on the NGO thickness. For the 8 uc thick NGO layer, the sheet resistance shows a steep upturn at $T_{dep} = 1070$ K. The 20 uc samples show a similar tendency, but the increase in resistance with increasing deposition temperature is much less pronounced.

For the 20 uc samples, the carrier density, n_S (Fig. 2(c)), decreases gradually with increasing T_{dep}, whereas the electron mobility, $\mu_n \approx 5\,\mathrm{cm}^2/\mathrm{Vs}$ (Fig. 2(d)), remains unaffected. For the thinner 8 uc samples, n_S shows an even stronger decrease from $1.1 \times 10^{14}\,\mathrm{cm}^{-2}$ (970 K) down to $3.5 \times 10^{13}\,\mathrm{cm}^{-2}$ (1070 K). μ_n varies around a mean value of about $5\,\mathrm{cm}^2/\mathrm{Vs}$ for the samples grown between 920 K and 1020 K. However, for $T_{dep} = 1070$ K, the mobility is significantly reduced ($\mu_n \approx 2\,\mathrm{cm}^2/\mathrm{Vs}$).

Although the cation stoichiometry is quite different for the samples grown between 920 K and 1020 K, their electrical properties at room temperature are remarkably similar. Conducting interfaces are found over a wide stoichiometry range. Only for a very low Ga content obtained at 1070 K, the sheet resistance is significantly increased.

An evaporation of Ga may primarily take place at the surface of the NGO film during and after the deposition. During growth, the Ga evaporation partially can be compensated by the oversaturated material supply within the subsequent plasma pulses. However, after growth and during cooling, the amount of Ga decreases continuously as long as the sample temperature is sufficiently high. Hence, the lack of Ga is rather more pronounced at the surface of the NGO film than close to the NGO/STO interface, resulting in a stoichiometry gradient. This is in agreement with the observation that all films initially grow in a similar layer-by-layer growth mode yielding a similar well-ordered interface and a similar mobility for any of the 20 uc samples. By contrast, the stoichiometry and defect structure not only at the NGO/STO interface but also within the entire NGO layer may be of importance for the interface reconstructions and the resulting carrier density.[14]

Considering a stoichiometry gradient, the effect of a Ga-deficient NGO surface layer on the electrical properties of the NGO/STO interface should increase when the distance between surface and interface, i.e., the layer thickness, is decreased. In fact, a more pronounced effect of T_{dep} was observed for the 8 uc samples as compared with the 20 uc samples. For the 8 uc samples, μ_n is reduced for $T_{dep} = 1070$ K indicating that the disordered Ga-deficient region extends into the interface region, thereby affecting not only the carrier density but also the electron mobility.

The NGO/STO heterostructures were also investigated by means of high temperature conductance measurements in equilibrium with the surrounding atmosphere (HTEC, see Ref. 15 for experimental details). With this method, any influence of residual growth-induced oxygen vacancies ($V_O^{\bullet\bullet}$) in the STO substrate on the observed electrical conductance of NGO/STO heterostructures can be determined.[15] Exploiting the temperature and pO_2 dependence of the interface conductance contribution, information about the fundamental chemical processes at the NGO/STO interface and the associated thermodynamic constants can be extracted.[6,15]

Fig. 3(a) shows the HTEC characteristics of a representative NGO/STO heterostructure (10 uc NGO, $T_{dep} = 970$ K) for equilibration temperatures of 850 K, 900 K, 950 K, and 1000 K. In this temperature range (above 750 K), the oxygen exchange reactions of both STO (Ref. 16) and NGO (Ref. 17) are activated. Therefore, any non-equilibrium concentration of PLD-induced $V_O^{\bullet\bullet}$ in the NGO/STO heterostructure—in particular in the STO substrate—strives for equilibrium. As a consequence, the HTEC characteristics of both NGO/STO heterostructure and STO substrate would be identical if the observed conductivity of NGO/STO heterostructures merely resulted from a simple reduction of the STO substrate bulk. However, a clear deviation from the conventional behavior of the bare STO substrate (shown for 950 K, open symbols) is observed for intermediate pO_2 values (10^{-18} bar $\lesssim pO_2 \lesssim 10^{-8}$ bar). This evidences an additional thermally stable conductance contribution deriving from the NGO/STO interface. Between 10^{-18} bar and 10^{-12} bar, the conductance contribution of the NGO/STO interface shows a plateau-like temperature and pO_2 independent behavior. A similar behavior has been reported for the LAO/STO system.[6,15] According to Refs. 6 and 15, this behavior can be attributed to the presence of donor-type states at the conducting interface. For the NGO/STO system, these may be provided by Nd intermixing, trapped oxygen vacancies, or electronic interface reconstructions. Taking into account the

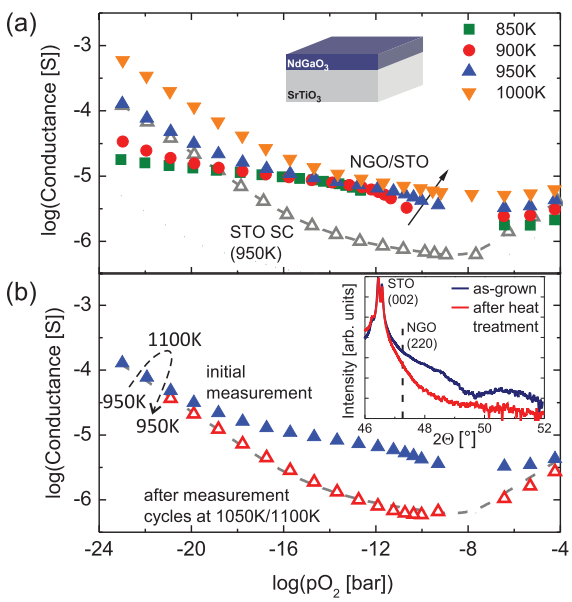

FIG. 3. HTEC characteristics of the NGO/STO heterostructure (filled symbols); (a) a thermally stable interface contribution is found for 850 K–1000 K; open symbols and dashed line correspond to the bare STO substrate (950 K); (b) comparison of the HTEC of the NGO/STO heterostructure at 950 K before (filled symbols) and after (open symbols) additional measurement cycles at 1050 K and 1100 K; the dashed line corresponds to STO single crystal data. (Inset: XRD data before and after the HTEC measurement.)

high temperature electron mobility in STO,[16] the conductance values of about 1×10^{-5} S in the plateau region correspond to an electron density of about 1×10^{14} cm^{-2}, which corresponds well with the carrier density measured at room temperature for as-grown samples (Fig. 2(c)). Between 10^{-12} bar and 10^{-8} bar, the conductance contribution of the NGO/STO interface decreases with increasing pO_2 and becomes thermally activated (indicated by the arrow in Fig. 3(a)). As proposed for the LAO/STO interface, this deviation from the conductance plateau can be related to an ionic charge compensation mechanism caused by the formation of Sr vacancies close to the conducting interface.[6]

Similar to the LAO/STO case,[6,15] the HTEC characteristics of the NGO/STO heterostructure can be described by the defect chemistry model of donor-doped STO up to 1000 K. However, when further increasing the equilibration temperature to 1050 K and 1100 K, an irreversible degradation of the interface conduction path takes place. Fig. 3(b) compares the HTEC characteristic of the NGO/STO heterostructure for 950 K obtained before (filled symbols) and after (open symbols) additional measurement cycles at 1050 K and 1100 K (corresponding to a heat treatment of several hours at various pO_2). The contribution of the interfacial conduction path disappeared after the thermal treatment, and the resulting HTEC characteristic of the high-temperature-treated NGO/STO heterostructure is identical with the characteristic of the STO substrate (dashed line). After cooling, the degraded heterostructure showed an insulating behavior and also structural modifications were observed. Comparing XRD data of the investigated sample before and after the thermal degradation, one finds a drastic change in the crystallinity of the NGO film. While clear thickness oscillations are found for the as-grown film, almost no indication for a crystalline perovskite layer can be found for the sample after the heat treatment (see inset of Fig. 3(b)). Moreover, XPS measurements on the degraded sample show that the Ga signal completely disappeared, whereas Nd was still well detectable. Hence, the NGO/STO heterostructure suffers from the same preferential evaporation of Ga during the HTEC measurement, which was observed for samples grown at various deposition temperatures. In fact, the temperature range where the irreversible process occurs in the HTEC measurement (1000 K–1100 K) corresponds well with the growth temperature range where NGO thin films tend to be strongly Ga-deficient (1020 K–1070 K). Due to a longer exposure time during the HTEC measurements, the effect is even more pronounced than during the variation of growth temperature. This results in a full depletion of Ga in the NGO layer accompanied with a change from initially conducting behavior to insulating behavior after the HTEC measurements above 1000 K. Thus, a sufficient Ga content within the NGO layer is essential not only to initialize but also to preserve the conductivity at the NGO/STO interface. Therefore, a simple implantation of Nd^{3+} donors into the STO substrate during growth—which should be independent of subsequent evaporation of Ga from the adjacent NGO film—most likely is not the predominant origin of the interface conduction.

In conclusion, it has been shown that the cation stoichiometry of NGO is of crucial importance for the structural and electrical properties of NGO/STO heterostructures. Due to the preferential evaporation of Ga during and after film growth, the Ga content in the NGO thin films can be altered by the choice of the PLD growth temperature. Conducting interfaces have been found over a wide stoichiometry range, while the sheet resistances of the heterostructures significantly increase as soon as the Ga content becomes too small. HTEC measurements show that the interface conduction degrades continuously during a heat treatment above 1000 K as an effect of Ga evaporation at elevated temperatures. The results indicate that the observed conductivity of the NGO/STO heterostructure originates neither from residual oxygen vacancies in the STO substrate nor from a mere implantation of Nd^{3+} ions during the growth process. Rather, the importance of the B-site cation in the NGO layer is emphasized. In general, NGO/STO heterostructures show interface reconstructions similar to the LAO/STO system as long as a proper crystallinity and a proper stoichiometry of the NGO thin films are maintained.

One of the authors (K.S.) acknowledges financial support by the Initiative and Networking Fund of the German Helmholtz Association, Helmholtz Virtual Institute VH-VI-442 MEMRIOX.

[1]A. Ohtomo and H. Y. Hwang, Nature **427**, 423 (2004).
[2]N. Nakagawa, H. Hwang, and D. Muller, Nature Mater. **5**, 204 (2006).
[3]G. Herranz, M. Basletić, M. Bibes, C. Carrétéro, E. Tafra, E. Jacquet, K. Bouzehouane, C. Deralot, A. Hamzic, J. M. Broto *et al.*, Phys. Rev. Lett. **98**, 216803 (2007).
[4]W. Siemons, G. Koster, H. Yamamoto, W. A. Harrison, G. Lucovsky, T. H. Geballe, D. H. A. Blank, and M. R. Beasley, Phys. Rev. Lett. **98**, 196802 (2007).
[5]S. A. Pauli and P. R. Willmott, J. Phys. Condens. Matter **20**, 264012 (2008).
[6]F. Gunkel, P. Brinks, S. Hoffmann-Eifert, R. Dittmann, M. Huijben, J. E. Kleibeuker, G. Koster, G. Rijnders, and R. Waser, Appl. Phys. Lett. **100**, 052103 (2012).
[7]P. Perna, D. Maccariello, M. Radovic, U. S. di Uccio, I. Pallecchi, M. Codda, D. Marre, C. Cantoni, J. Gazquez, M. Varela *et al.*, Appl. Phys. Lett. **97**, 152111 (2010).
[8]Y. Hotta, T. Susaki, and H. Y. Hwang, Phys. Rev. Lett. **99**, 236805 (2007).
[9]U. S. di Uccio, C. Aruta, C. Cantoni, E. D. Gennaro, and A. Gadaleta, "Reversible and persistent photoconductivity at the $NdGaO_3/SrTiO_3$ conducting interface," e-print arXiv:1206.5083v1 (unpublished).
[10]R. Dirsyte, J. Schwarzkopf, G. Wagner, J. Lienemann, M. Busch, H. Winter, and R. Fornari, Appl. Surf. Sci. **255**, 8685–8687 (2009).
[11]E. Talik, A. Kruczek, H. Sakowska, Z. Ujma, M. Gala, and M. Neumann, J. Alloys Compd. **377**, 259–267 (2004).
[12]S. Thiel, G. Hammerl, A. Schmehl, C. W. Schneider, and J. Mannhart, Science **313**, 1942 (2006).
[13]A. Brinkman, M. Huijben, M. van Zalk, J. Huijben, U. Zeitler, J. C. Maan, W. G. van der Wiehl, G. Rijnders, D. H. A. Blank, and H. Hilgenkamp, Nature Mater. **6**, 493 (2007).
[14]M. Reinle-Schmitt, C. Cancellieri, D. Li, D. Fontaine, M. Medarde, E. Pomjakushina, C. W. Schneider, S. Gariglio, P. Ghosez, J. M. Triscone, and P. R. Willmott, Nature Commun. **3**, 932 (2012).
[15]F. Gunkel, S. Hoffmann-Eifert, R. Dittmann, S. B. Mi, C. L. Jia, P. Meuffels, and R. Waser, Appl. Phys. Lett. **97**, 012103 (2010).
[16]R. Moos and K. H. Haerdtl, J. Am. Ceram. Soc. **80**, 2549 (1997).
[17]T. Ishihara, H. Matsuda, M. A. bin Bustam, and Y. Takita, Solid State Ionics **86–88**, Part 1, 197 (1996).